Supplementary Material:

Supplementary Figure 1. Characterization of the analysed K8 variants. (A) The conservation of K8 G62 and K8 R341 residues was compared among selected species. The figures were prepared using the following reference sequences: K8: NM 002273.3 (*Homo sapiens*), NM 19937.1 (*Rattus norvegicus*), NM 031170.2 (*Mus musculus*), BC 044116.1 (*Xenopus laevis*). Single letter abbreviations represent the respective amino acids. **(B)** Representative DNA sequences (forward direction only) depict an unaltered K8 sequence in mice overexpressing wild type human K8 (WT K8) whereas animals carrying K8 variants display following point mutations: K8 G62C: GGC→TGC in K8 exon 1; K8 R341H/C: CGT→CAT/TGT in K8 exon 6.

Supplementary Figure 2. Overexpression of keratin 8 variants does not affect keratin network alteration. Livers from transgenic mice overexpressing wild type human (h) keratin 8 (WT K8), hK8 G62C or K8 R341C/H variant and tissues from nontransgenic animals (FVB/N) were stained with an antibody recognizing both mouse and human K8/K18 (8592) or an antibody detecting only human K8 (M20). Scale bar = 50 μm.

Supplementary Figure 3. RT-PCR analysis quantified the expression of Dpt **(A)** and Tubb2a **(B)** in mice overexpressing wild type K8 (WT K8) or the highlighted K8 variants. L7 (mouse ribosomal protein) gene was used as an internal control. At least four mice were analysed per genotype and the results are expressed mean ±SEM.

Supplementary Figure 4. Relationship between K8/K18 expression and nicotinamide N-methyltransferase (NNMT) levels. (A-D). NIH-3T3 cells were transfected with empty vector (mock) or with K8+K18 cDNA (transfected), lysed and subjected to RT-PCR analysis (A-C) or to immunoblotting (D). L7 (mouse ribosomal protein) and actin were used as an internal/loading control for RT-PCR and immunoblotting, respectively. **(E)** NNMT mRNA levels were also quantified in liver extracts from K18-deficient (K18 KO) animals and their

non-transgenic littermates (WT). L7 (mouse ribosomal protein) was used as an internal control for qRT-PCR. At least 4 mice were analysed per genotype. *p<0.05, **p<0.01.

Supplementary Figure 5. Loss of K18 does not alter the susceptibility to acetaminophen-induced liver injury. Non-transgenic animals (WT) and mice lacking K18 (K18 KO) were injected with 600mg/kg acetaminophen (APAP) intraperitoneally and sacrificed 18h thereafter. **(A)** Both mouse strains display comparable serum alanine aminotransferase (ALT) levels. **(B)** H&E staining detected marked hepatocyte swelling and necrosis. While the overall extent of liver injury was comparable in both strains (as confirmed by morphometric analysis with the scores being WT: 2.9 ±0.9 and K18 KO 3.3±0.6), the liver injury in K18 WT mice was more restricted to the central area whereas K18 KOs displayed a more ubiquitous liver injury pattern. Results are presented as mean ± SEM and least 7 mice were analysed per genotype. Scale bar=50 μm

Supplementary Figure 6. Presence of K8 variants does not affect the APAP metabolism. APAP plasma concentration was measured in mice overexpressing wild type K8 (WT K8) or K8 variants four hours after intraperitoneal administration of 600mg/kg APAP. Boxplots display median with first and third percentile, while whiskers indicate smallest and largest non-outlier observations. At least ten mice were analysed per genotype.

Supplementary Figure 7. Presence of K8 G62C and R341C variants did not affect the expression of genes associated with acetaminophen metabolism. mRNA levels of APAP metabolism-related cytochrome genes Cyp2e1 **(A),** Cyp1a2 **(B)** and a GSH biosynthesis-related gene Gstp1 were determined in untreated mice by qRT-PCR. **(D)** Immunoblotting was used to quantify Cyp2e1 protein levels in mice exposed to APAP for four hours. L7 (mouse ribosomal protein) gene and actin were used as an internal control/loading control for qRT-PCR and immunoblotting, respectively. Results are presented as mean ± SEM (n=5 per genotype).

Supplementary Fig. 8. Glutathione levels and APAP-mediated inflammation/apoptosis is not altered by presence of K8 variants. To study the impact of overexpression of wild type human K8 (WT K8) or K8 variants on APAP-induced liver injury, total hepatic glutathione **(A)** and the ratio of oxidized to reduced glutathione (GSSG/GSH) **(B)** was measured at basal conditions and 4h after APAP administration. Plasma levels of IL-6 **(C)** and TNFα **(D)** cytokines were determined as markers of hepatic inflammation, whereas ATP levels assessed the hepatic energy status **(E)**. At least five mice were analysed per genotype and the results are expressed mean ± SEM. Cleaved caspase 3 and a caspase-cleaved K18 fragment that constitute established apoptosis markers were detected in total liver lysates by immunoblotting **(F)**. Note that only low levels of apoptotic markers were seen in all genotypes. Actin was used as a loading control.

Supplementary Figure 9. Mice carrying K8 variants display pericentral keratin network disruption. Mice overexpressing wild type K8 (WT K8) or K8 G62C/ R341H variants were treated with APAP for 18 hours and the liver sections were stained with a combination of K8/K18 antibody (green) and an antibody recognizing phosphorylated (p) K8 (red). Note pericentral K8 hyperphosphorylation and keratin network disruption in mice carrying human K8 variants. Scale bar=50 μm

Supplementary Figure 10. Overexpression of K8 G62C/R341H variants does not affect the development of bile duct ligation (BDL)-induced cholestatic liver injury. H&E-stained liver sections demonstrate the presence of BDL-induced ductal proliferation as well as periportal inflammation (d-f), however their extent did not differ significantly between animals overexpressing wild type K8 (WT K8; a,d) and mice carrying K8 variants (b,c,e,f). Untreated animals (a-c) did not display apparent alterations in liver architecture irrespectively of their genotype. Scale bar= 100 μm.

Supplementary Table 1. Primers used for genotyping, sequencing and qRT-PCR

Primers	**Sequence**
Genotyping primers *(Human KRT8)*	F:GGCGGCGGCTATGGTGGGGCC R:AGATGTGCATAGGGACCGGGA
Sequencing primers *(KRT8, Exon 1)*	F:TGCCTCTACCATGTCCATCA R:CGGGACTACCAGGAGAAAGG
Sequencing primers *(KRT8, Exon 6)*	F:CATACCCAACCTGACCTACTTACC R:AGAACAACAGGACCCCAAGTC
Primers for qRT-PCR	
Mouse cytochrome P450 1a2 *(Cyp1a2)*	F:TCTGCCAGTCTCCAGCCCCT R:AGATGGCAGTGGCCAGTAGCA
Mouse cytochrome P450 2e1 *(Cyp2e1)*	F:CTGGCCGAGGGGACATTCCTGT R:AGGGAAAACCTCCGCACGTCCT
Mouse glutathione S-transferase Pi gene *(Gstp1)*	F:GGGCCAGAGCTGGAAGGAGGA R:CCTCAAACTTGGGGAGCTGCCC
Mouse collagen, type I, alpha 1 *(Cola1a)*	F:TGAAGAACTGGACTGTCCCAACC R:GGGTCCCTCGACTCCTACATCTT
Mouse keratin 8 *(Krt8)*	F:GGACATCGAGATCACCACCT R:TGAAGCCAGGGCTAGTGAGT
Mouse keratin 18 *(Krt18)*	F:CAAGTCTGCCGAAATCAGGGAC R:TCCAAGTTGATGTTCTGGTTTT
Human keratin 8 *(KRT8)*	F:GCTGACCGACGAGATCAACT R:CATGGACAGCACCACAGATG
Human keratin 18 *(KRT18)*	F:ACAGTCTGCTGAGGTTGGAGCT R:TCCAAGCTGGCCTTCAGATTTC
Mouse nicotinamide N-methyltransferase *(Nnmt)*	F:GGCTTCCTGGTGATGGTAGA R:TTCCACAGCATCTCGAACAG
Mouse dermatopontin (Dpt)	ATATGCGAGGAGCAACAACC CGAATTCGCAGTCGTAGTCA
Mouse reticulocalbin 2 (Rcn2)	GTACGACCGGGTGATTGACT TGCTCAAACGCAATGAACTC
Mouse Glucokinase (Gck)	AAAGATGTTGCCCACCTACG GCATCACCCTGAAGTTGGTT
Mouse Tubulin Beta 2a (Tubb2a)	CTCCACCCCTTCTACAACCA TCCAGCTGCAAGTCACTGTC
Mouse ribosomal protein (*L7*)	F:GAAAGGCAAGGAGGAAGCTCATCT R:AATCTCAGTGCGGTACATCTGCCT

Supplementary Table 2. Genes differentially expressed in K8 G62C and WT K8 mouse livers

Gene symbol	Description	Parametric p-value	Fold-change G62C/WT K8
Hspa1a	heat shock protein 1A	0.0372152	2.1910079
Hspa1b	heat shock protein 1B	0.0257361	2.0498078
Cyp4a14	cytochrome P450, family 4, subfamily a, polypeptide 14	0.0026926	2.041079
Dpt	dermatopontin	0.0088491	1.9783376
Zbtb16	zinc finger and BTB domain containing 16	0.0457761	1.9445693
Nr0b2	nuclear receptor subfamily 0, group B, member 2	0.0293455	1.7760128
Aph1c	anterior pharynx defective 1c homolog (C. elegans)	0.0003751	1.7340112
Slc30a10	solute carrier family 30, member 10	0.0101304	1.7244651
Tubb2a	tubulin, beta 2a	0.0237996	1.6947036
Vapb	vesicle-associated membrane protein, associated protein B and C	0.0006812	1.6696454
2410076I21Rik	RIKEN cDNA 2410076I21 gene	0.0313241	1.6297332
Clpx	caseinolytic peptidase X (E.coli)	0.0069996	1.6112241
Arntl	aryl hydrocarbon receptor nuclear translocator-like	0.0185035	1.5746843
Dnaic1	dynein, axonemal, intermediate chain 1	0.0058982	1.5742695
Accn5	amiloride-sensitive cation channel 5, intestinal	0.0178268	1.5709451
Arih1	ariadne ubiquitin-conjugating enzyme E2 binding protein homolog 1 (Drosophila)	0.0016032	1.5685961
Cdkn1a	cyclin-dependent kinase inhibitor 1A (P21)	0.013185	1.5166108
Tacc2	transforming, acidic coiled-coil containing protein 2	0.0002771	1.51391
Per3	period homolog 3 (Drosophila)	0.0128328	0.6644887
Stard4	StAR-related lipid transfer (START) domain containing 4	0.0085884	0.6643053
Erdr1	erythroid differentiation regulator 1	0.0051957	0.659464
Cxcl1	chemokine (C-X-C motif) ligand 1	0.015433	0.6546569
Cyp2a5	cytochrome P450, family 2, subfamily a, polypeptide 5	0.0095557	0.6525306
Mid1ip1	Mid1 interacting protein 1 (gastrulation specific G12-like (zebrafish))	0.0120402	0.6513541
Nsdhl	NAD(P) dependent steroid dehydrogenase-like	0.0313168	0.6505928
D0H4S114	DNA segment, human D4S114	0.0112636	0.6498561
Wee1	WEE 1 homolog (S. pombe)	0.0175853	0.6461879
Sfrs5	splicing factor, arginine/serine-rich 5 (SRp40, HRS)	0.0285332	0.6442628
Dclre1a	DNA cross-link repair 1A, PSO2 homolog (S. cerevisiae)	0.0228872	0.6424867
Insig1	insulin induced gene 1	0.0374667	0.6409023
Onecut1	one cut domain, family member 1	0.002869	0.6375468
S100a8	S100 calcium binding protein A8 (calgranulin A)	0.0049793	0.6176464

Pcsk9	proprotein convertase subtilisin/kexin type 9	0.0023724	0.6014568
Serpina7	serine (or cysteine) peptidase inhibitor, clade A (alpha-1 antiproteinase, antitrypsin), member 7	0.0067962	0.5986233
Alas1	aminolevulinic acid synthase 1	0.0450874	0.581037
Mafb	v-maf musculoaponeurotic fibrosarcoma oncogene family, protein B (avian)	0.0128553	0.5719413
Fdps	farnesyl diphosphate synthetase	0.0411368	0.5658987
Dbp	D site albumin promoter binding protein	0.014511	0.5525418
Nnmt	nicotinamide N-methyltransferase	0.0386286	0.5472025
Idi1	isopentenyl-diphosphate delta isomerase	0.0240344	0.5328265
Cyp51	cytochrome P450, family 51	0.0246763	0.5270043
Sc5d	sterol-C5-desaturase (fungal ERG3, delta-5-desaturase) homolog (S. cerevisae)	0.000017	0.5222336
4432416J03Rik	RIKEN cDNA 4432416J03 gene	0.0022453	0.4825756
Sqle	squalene epoxidase	0.0141237	0.4702062
Sc4mol	sterol-C4-methyl oxidase-like	0.013992	0.4449625
Cyp7a1	cytochrome P450, family 7, subfamily a, polypeptide 1	0.0002588	0.4104663
Rcn2	reticulocalbin 2	0.0000222	0.4093394

Supplementary Table 3. Genes differentially expressed in K8 R341H and WT K8 mouse livers

Gene symbol	Description	Parametric p-value	Fold-change R341H/WT K8
Car3	carbonic anhydrase 3	0.0056876	2.6086401
Arrdc3	arrestin domain containing 3	0.0198644	2.3418892
Mpa2l	macrophage activation 2 like	0.0030948	2.1886423
Gck	glucokinase	0.0001276	1.8887603
Raet1a	retinoic acid early transcript 1, alpha	0.0139628	1.8025588
5830443L24Rik	RIKEN cDNA 5830443L24 gene	0.0298334	1.7826253
Aph1c	anterior pharynx defective 1c homolog (C. elegans)	0.0002243	1.7794398
2410076I21Rik	RIKEN cDNA 2410076I21 gene	0.0380272	1.7216223
Col3a1	collagen, type III, alpha 1	0.0253261	1.7148381
Cyp51	cytochrome P450, family 51	0.0404575	1.6732479
Serpina6	serine (or cysteine) peptidase inhibitor, clade A, member 6	0.0364276	1.6570368
Aqp8	aquaporin 8	0.0497801	1.6497728
Stom	stomatin	0.0000073	1.612592
LOC100040592	similar to Hmgcs1 protein	0.011545	1.6049693
Arhgap6	Rho GTPase activating protein 6	0.0017328	1.6015749
Srebf1	sterol regulatory element binding transcription factor 1	0.0029853	1.5937282
LOC100040592	similar to Hmgcs1 protein	0.0133211	1.5918012
Dpt	dermatopontin	0.0290332	1.5898551
Apol9a	apolipoprotein L 9a	0.0000021	1.5697549
Ntrk2	neurotrophic tyrosine kinase, receptor, type 2	0.032892	1.5686477

Rab8b	RAB8B, member RAS oncogene family	0.0009081	1.5438771
Gna14	guanine nucleotide binding protein, alpha 14	0.0006017	1.5335074
Sox4	SRY-box containing gene 4	0.0169844	1.5323062
9030411M13Rik	RIKEN cDNA 9030411M13 gene	0.0135733	1.5312402
Inhbe	inhibin beta E	0.0302958	1.5261802
Efna1	ephrin A1	0.0489881	1.52152
LOC100040592	similar to Hmgcs1 protein	0.0150011	1.5208938
Lss	lanosterol synthase	0.0433299	1.5038956
Mfsd2	major facilitator superfamily domain containing 2	0.0446817	0.6606487
A130040M12Rik	RIKEN cDNA A130040M12 gene	0.0045216	0.6506759
Syt11	synaptotagmin XI	0.0000102	0.6503278
A130040M12Rik	RIKEN cDNA A130040M12 gene	0.0007782	0.648019
Mafb	v-maf musculoaponeurotic fibrosarcoma oncogene family, protein B (avian)	0.0254995	0.628809
Errfi1	ERBB receptor feedback inhibitor 1	0.0217811	0.6247024
Onecut1	one cut domain, family member 1	0.0001261	0.6037764
Lpin1	lipin 1	0.0214228	0.5915586
Rasgef1b	RasGEF domain family, member 1B	0.0059452	0.5653982
1110004O12Rik	RIKEN cDNA 1110004O12 gene	0.0011837	0.5405064
AI842396	expressed sequence AI842396	0.0000019	0.5396685
Igfbp1	insulin-like growth factor binding protein 1	0.0336297	0.5320721
Ctgf	connective tissue growth factor	0.0151655	0.5209069
Got1	glutamate oxaloacetate transaminase 1, soluble	0.0098622	0.5166222
Sult1e1	sulfotransferase family 1E, member 1	0.0361067	0.4808185
Wsb1	WD repeat and SOCS box-containing 1	0.0028801	0.4793133
Rcn2	reticulocalbin 2	0.000133	0.4525833
Nnmt	nicotinamide N-methyltransferase	0.0000497	0.231202

Supplementary methods:

Histological and immunofluorescence staining

Paraformaldehyde-fixed, paraffin embedded samples were cut into 3-5 µm thin sections and stained with haematoxylin and eosin (H&E) or picro-sirius red (PSR). Images were acquired on a Leica light microscope with digital camera (Model DM 5500, Leica Microsystems Imaging Solutions GmbH, Wetzlar, Germany) and the appropriate software (Leica Application Suite 3.8). For immunofluorescence staining, liver pieces were frozen in pre-cooled methylbutane, fixed in acetone, cut into 2µm thick slides (S1) and incubated with following primary antibodies overnight at 4°C: human K8 (C5301; Sigma, Munich, Germany), K8/K18 (8592; (S2) or phosphorylated (p) K8 S74/S432 recognizing both the

human pK8 S74/S432 and the analogous mice pK8 S80/S438 phospho-sites (LJ4/5B3; (S3-5). Slides were washed with 0.1% Tween-20-containing Tris Base saline buffer (TBST), exposed to the appropriate fluorescent dye-conjugated secondary antibody and mounted in the ProLong Gold antifade mounting medium containing DAPI for nuclei staining (Invitrogen/Life Technologies).

To evaluate the APAP hepatotoxicity, H&E-stained liver sections were scored by two independent observers as: 0, no obvious pathology; 1, mild hepatocyte swelling/inflammation/no necrosis; 2, moderate swelling/beginning necrosis; 3, distinct necrosis/small hemorrhagic areas; 4, prominent necrosis/large hemorrhagic areas.

To quantify keratin network disruption, K8/K18-stained liver sections were scored as: 0, normal appearing network; 1/2/3, a few/frequent/abundant cells with disrupted keratin network.

cDNA translation and quantitative reverse transcriptase PCR (qRT-PCR) analysis

Total RNAs was obtained using the RNeasy tissue mini isolation kit (Qiagen, Hilden, Germany) and qRT-PCR was performed with Sequence Detection System (Applied Biosystems 7500 fast Real Time PCR system). The RNA samples were translated to cDNAs with Superscript II reverse transcriptase kit and oligo-dT primers (Invitrogen). The relative expression of genes of interest was determined using specific primers (Supplementary Table 1). Mouse L7 (ribosomal RNA) was employed as internal control.

Cell culture experiments

To study the impact of K8/K18 expression on NNMT levels, NIH-3T3 cells (mouse fibroblast CRL-1658; American Type Culture Collection) were grown to 90-95% confluency in DMEM medium (Gibco, Life Technologies GmbH, Darmstadt, Germany) supplemented with 10% FCS, 1% penicilin-streptomycin and 1% L-Glutamine, then transfected with equal amounts of human K8 and K18 DNA using Lipofectamine 2000 (Invitrogen, Life Technologies GmbH, Darmstadt, Germany). 24 hours after transfection, the cells were either lysed with RNeasy

mini isolation kit or with 3% sodium dodecyl sulphate (SDS)-containing buffer in order to obtain total RNA and total protein lysate, respectively.

Microarray Analysis:

Microarray analyses were performed in Microarray Chip Facility Unit at University of Ulm as described previously (S6). Four females and four males (all two months old) were analysed per genotype. Briefly, 200ng of total RNA was amplified and labeled as described in the Whole Transcript (WT) Sense Target Labeling Assay (GeneChip Fluidics Station 450; Affymetrix, Santa Clara, CA). Labeled ssDNA was hybridized to Mouse Gene 1.0 ST Affymetrix GeneChip arrays (Affymetrix) and after scanning, the images were analyzed using Affymetrix® Expression Console™ Software (Affymetrix). Genes with a *P* value less than 0.05 and displaying at least 1.5 fold alteration between the genotypes were used for the further analysis. Complete microarray data are available at Gene Expression Omnibus (GEO accession number pending).

Protein biochemistry

Liver tissues were homogenized in a 3% sodium dodecyl sulphate (SDS)-containing buffer and in most instances diluted in 4x reducing Laemmli buffer. Non-reducing Laemmli buffer was used for analysis of disulfide cysteine bridges. To obtain soluble keratins, samples were first homogenized in a 1% Triton X-containing buffer and pellets were dissolved in 3% SDS buffer. Alternatively, protein extracts enriched in insoluble keratins were prepared via high salt extraction (HSE; (S2)). For immunoprecipitation, HepG2 (ATCC No.HB-8065) or Huh7 (ATCC No. CCL-185) cells were grown to 80% confluency, scraped in cold PBS and centrifuged. The lysates were prepared using 1% NP 40/PBS-EDTA with protease inhibitors as the lysis buffer. L2A1 (anti-K18) antibody was conjugated to protein G Dynabeads (Invitrogen), which was then incubated with the NP40 lysates as recommended by the supplier. Eluted samples were diluted in 4x non reducing Laemmli buffer. Proteins were separated by SDS-PAGE, transferred to membranes and incubated with the following

antibodies: hK8 (C5301; Sigma), m,hK18 (4668; (S7), human K18 (L2A1; (S8), K8/K18 (8592; (S2), JNK1 (3708; Cell Signaling, Danvers, MA), JNK2 (sc-827, Santa Cruz), pJNK (9251S; Cell Signaling), phospho-p38 (9211S; Cell Signaling), Cyp2e1 (19140, Abcam, Cambridge, UK), K18 apoptotically cleaved at D238 (5148A5 termed also as D238; AnaSpec, Fremont, CA), caspase 3 (ab2302; Abcam, Cambridge, UK) and beta-actin (A1978; Sigma); NNMT (PA5-11143, Thermo) Secondary, horseradish peroxidase-conjugated antibodies were used (Life Technologies) and the proteins were visualized by enhanced chemiluminescence (RPN2106/ RPN2236; GE Healthcare Amersham Buckinghamshire, UK). Extracts obtained via HSE were stained with SYPRO ruby (50562; Lonza, Basel, Switzerland) as recommended by the supplier and visualized under UV light.

Biochemical and cytokine assays

The amount of total glutathione and the ratio of oxidized to reduced glutathione (GSSG/GSH) was measured using a commercial kit (Cayman Chemical Co, Ann Arbor, MI) as recommended by the manufacturer. For determination of ATP levels, livers were perfused with a phosphate-buffered saline (PBS) in situ to remove blood. 100 mg of tissue was boiled in distilled water for 10 minutes, chilled shortly on ice and homogenized using the Potter-Elvehjem grinder with Teflon pestle. ATP concentration was measured with the ATPlite assay (Perkin Elmer, Waltham, MA) according to manufacturer's instructions.

To quantify the amount of APAP-protein adducts, 100 mg of liver tissue was homogenized in ice cold PBS and digested with protease. Small molecules were removed by gel-filtration on centrifugal desalting columns equilibrated with PBS, pH 7.2 (exclusion volume > 6,000 daltons). The excluded, putatively modified, proteins were analyzed for the presence of APAP-protein adducts after enzymatic digestion using high pressure liquid chromatography with electrochemical detection (HPLC-EC) of APAP-Cys as previously described (S9). In all

assays, protein content was determined with a Bradford assay and results were normalized based on protein concentration.

Serum concentrations of interleukin 6 (IL-6) and tumour necrosis factor α (TNFα) were determined using commercially-available ELISAs (M6000B/MTA00B; R&D, Minneapolis, MN). The concentration was measured as absorbance at 450 nm with wavelength correction at 540 nm.

Statistical Analysis

Based on the results of a normality test, a parametric 1-way ANOVA with Newman-Keuls post hoc test or non-parametric 1-way ANOVA with Kruskal-Wallis post hoc test were used. Two-tailed t-test was used for a comparison between two groups (such as between K18 KOs and WTs). A p-value < 0.05 was considered statistically significant.

Supplementary references:

S1. Ku NO, Toivola DM, Zhou Q, Tao GZ, Zhong B, Omary MB. Studying simple epithelial keratins in cells and tissues. Methods Cell Biol 2004;78:489-517.

S2. Ku NO, Michie S, Oshima RG, Omary MB. Chronic hepatitis, hepatocyte fragility, and increased soluble phosphoglycokeratins in transgenic mice expressing a keratin 18 conserved arginine mutant. J Cell Biol 1995;131:1303-1314.

S3. Ku NO, Michie SA, Soetikno RM, Resurreccion EZ, Broome RL, Omary MB. Mutation of a major keratin phosphorylation site predisposes to hepatotoxic injury in transgenic mice. J Cell Biol 1998;143:2023-2032.

S4. Liao J, Ku NO, Omary MB. Stress, apoptosis, and mitosis induce phosphorylation of human keratin 8 at Ser-73 in tissues and cultured cells. J Biol Chem 1997;272:17565-17573.

S5. Ku NO, Omary MB. Phosphorylation of human keratin 8 in vivo at conserved head domain serine 23 and at epidermal growth factor-stimulated tail domain serine 431. J Biol Chem 1997;272:7556-7564.

S6. Sunami Y, Leithauser F, Gul S, Fiedler K, Guldiken N, Espenlaub S, Holzmann KH, et al. Hepatic activation of IKK/NFkappaB signaling induces liver fibrosis via macrophage-mediated chronic inflammation. Hepatology 2012;56:1117-1128.

S7. Ku NO, Liao J, Omary MB. Phosphorylation of human keratin 18 serine 33 regulates binding to 14-3-3 proteins. EMBO J 1998;17:1892-1906.

S8. Liao J, Lowthert LA, Ku NO, Fernandez R, Omary MB. Dynamics of human keratin 18 phosphorylation: polarized distribution of phosphorylated keratins in simple epithelial tissues. J Cell Biol 1995;131:1291-1301.

S9. Muldrew KL, James LP, Coop L, McCullough SS, Hendrickson HP, Hinson JA, Mayeux PR. Determination of acetaminophen-protein adducts in mouse liver and serum and human serum after hepatotoxic doses of acetaminophen using high-performance liquid chromatography with electrochemical detection. Drug Metab Dispos 2002;30:446-451.

A.

Species	Sequence (G62C)
Homo sapiens	G **G** A S G M G **G** I T A V T V N Q
Mus musculus	F **G** G A G V G **G** I T A V T V N Q
Rattus norvegicus	F **G** G A G V G **G** I T A V T V N G
Xenopus laevis	G A G V G S A **G** I T S V S V N Q

Species	Sequence (R341C/H)
Homo sapiens	A A I A D A E Q **R** G E L A I K D
Mus musculus	A A I A D A E Q **R** G E M A I K D
Rattus norvegicus	A A I A D A E Q **R** G E L A V K D
Xenopus laevis	E L D A L K A Q **R** A N L E A Q I

B.

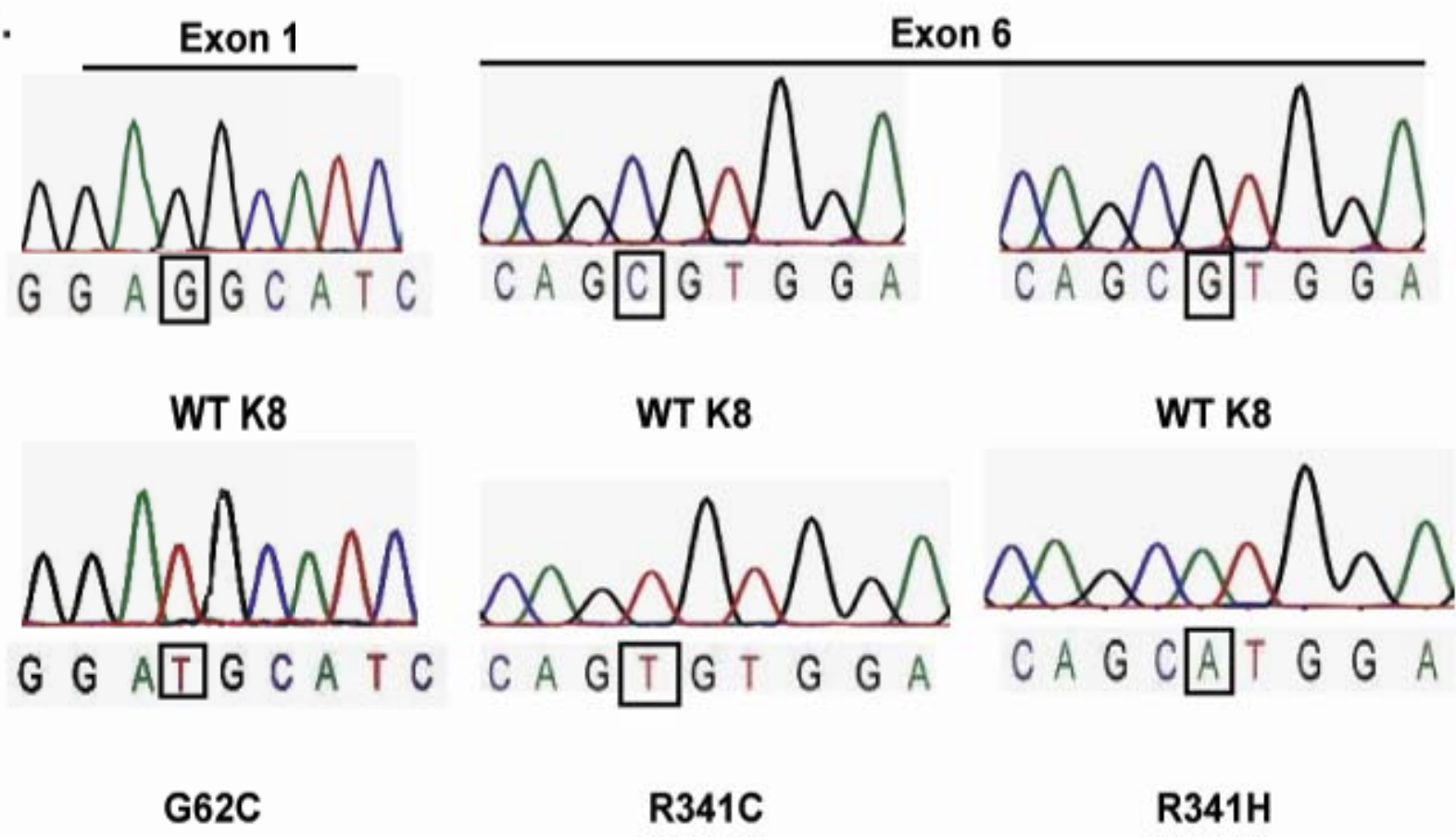

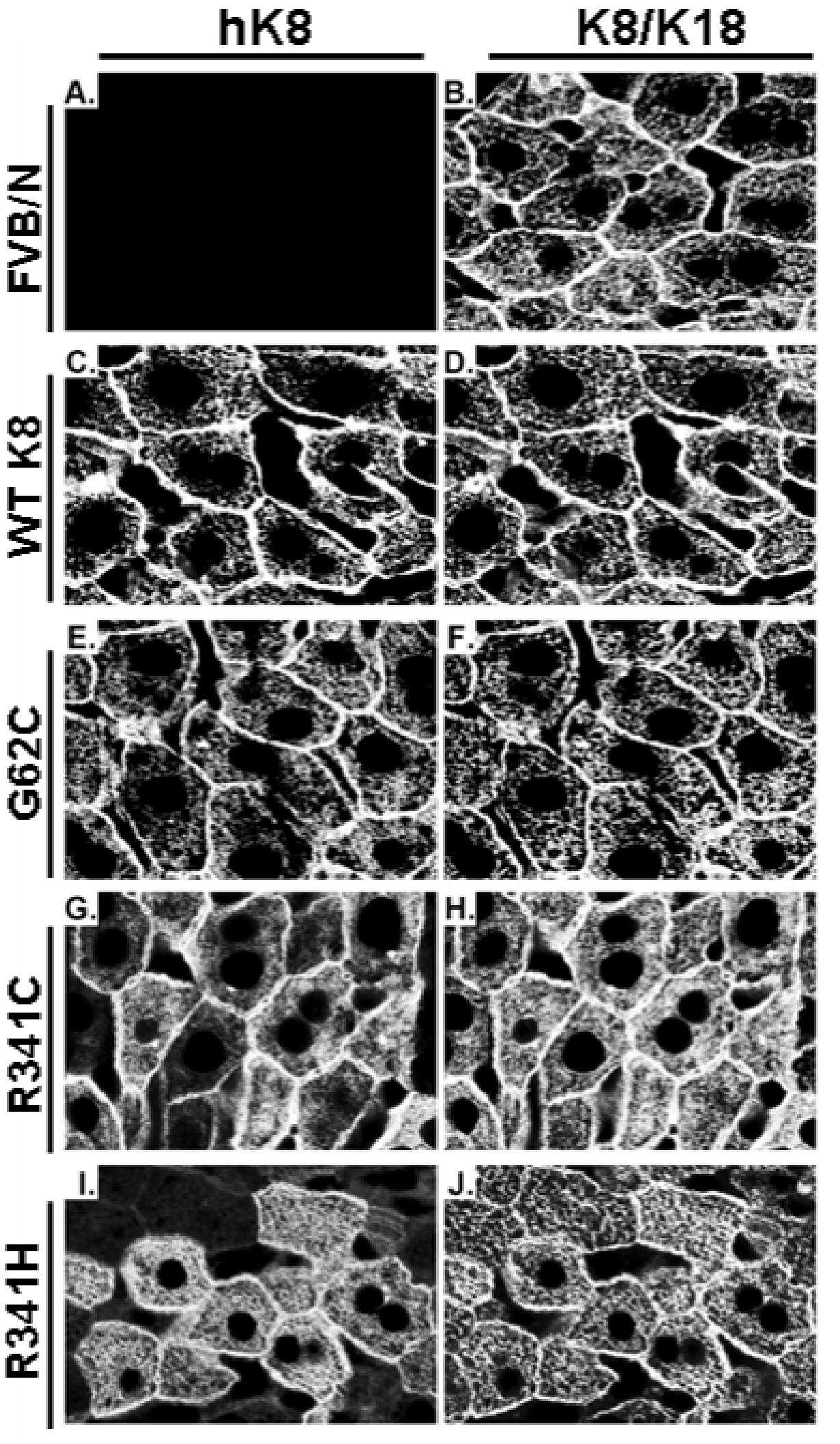
hK8
K8/K18
A.
B.
FVB/N
C.
D.
WT K8
E.
F.
G62C
G.
H.
R341C
I.
J.
R341H

A.

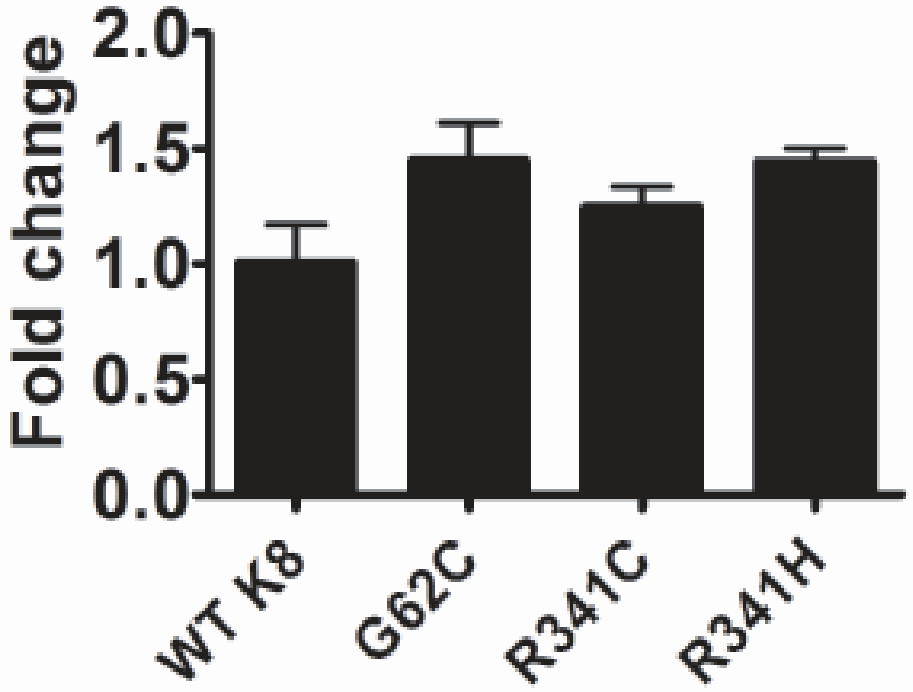
Dpt mRNA
Fold change
2.0
1.5
1.0
0.5
0.0
WT K8
G62C
R341C
R341H

B.

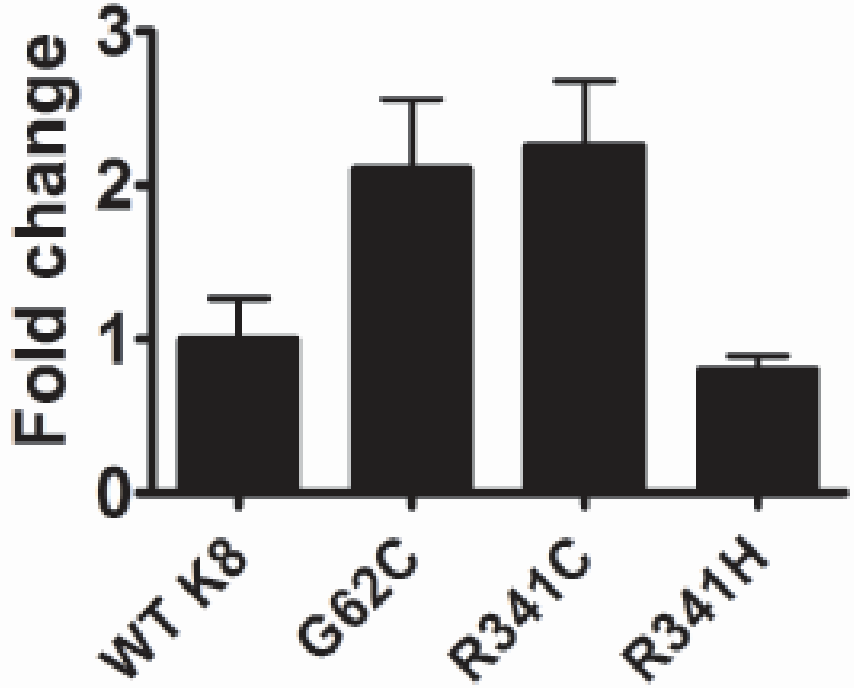
Tubb2a mRNA
Fold change
3
2
1
0
WT K8
G62C
R341C
R341H

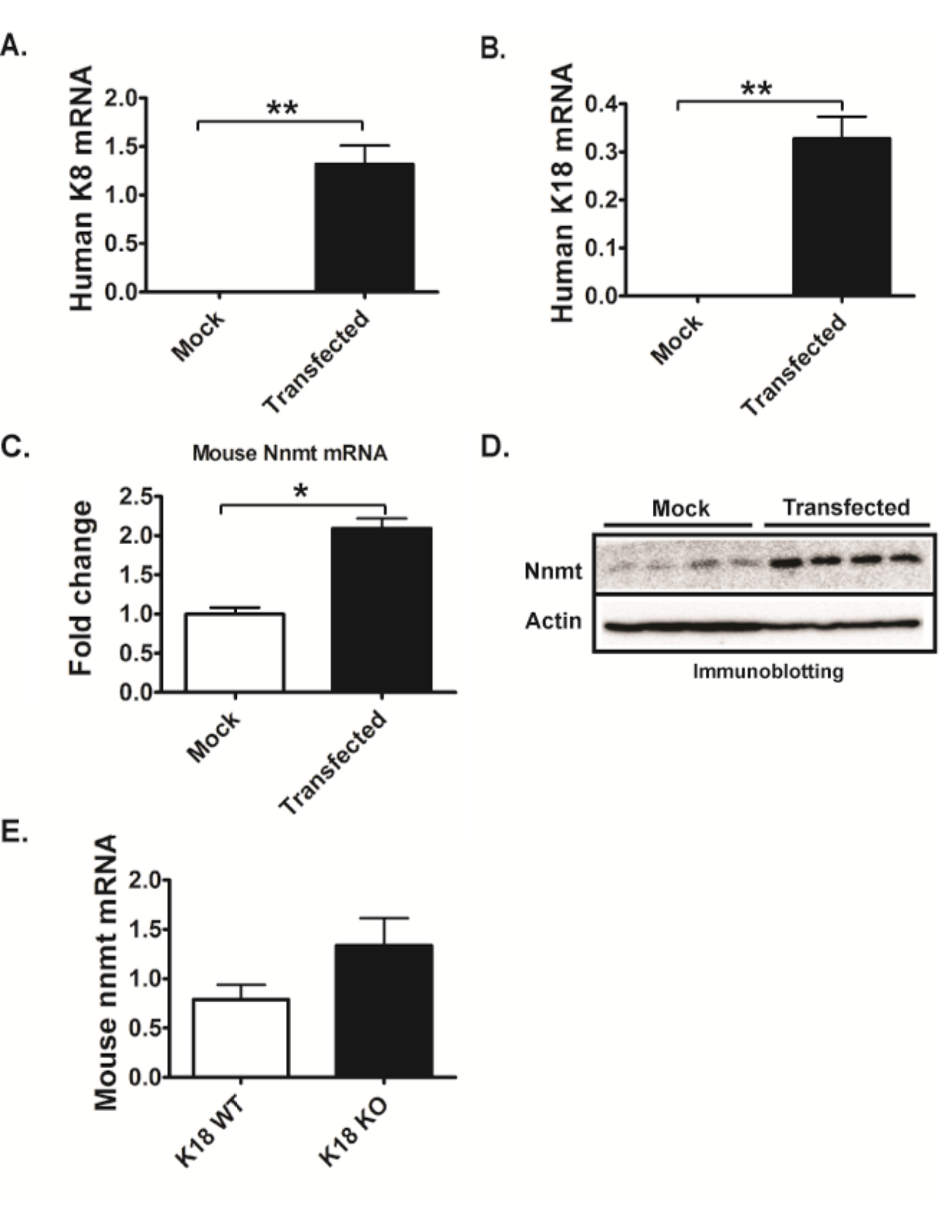
A.
Human K8 mRNA
2.0
1.5
1.0
0.5
0.0
**
Mock
Transfected
B.
Human K18 mRNA
0.4
0.3
0.2
0.1
0.0
**
Mock
Transfected
C.
Mouse Nnmt mRNA
Fold change
2.5
2.0
1.5
1.0
0.5
0.0
*
Mock
Transfected
D.
Mock
Transfected
Nnmt
Actin
Immunoblotting
E.
Mouse nnmt mRNA
2.0
1.5
1.0
0.5
0.0
K18 WT
K18 KO

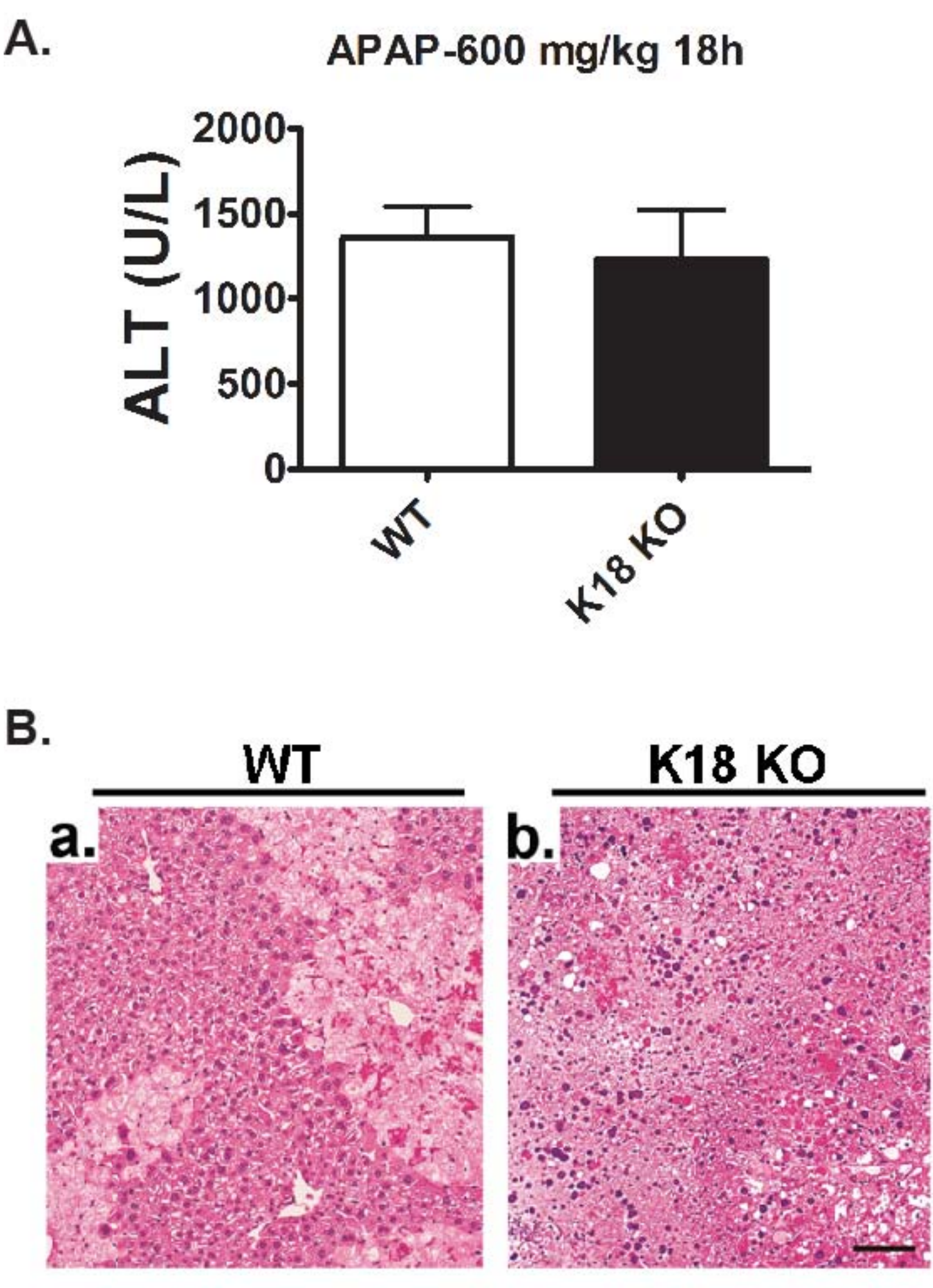
A.
APAP-600 mg/kg 18h
ALT (U/L)
2000
1500
1000
500
0
WT
K18 KO
B.
WT
K18 KO
a.
b.

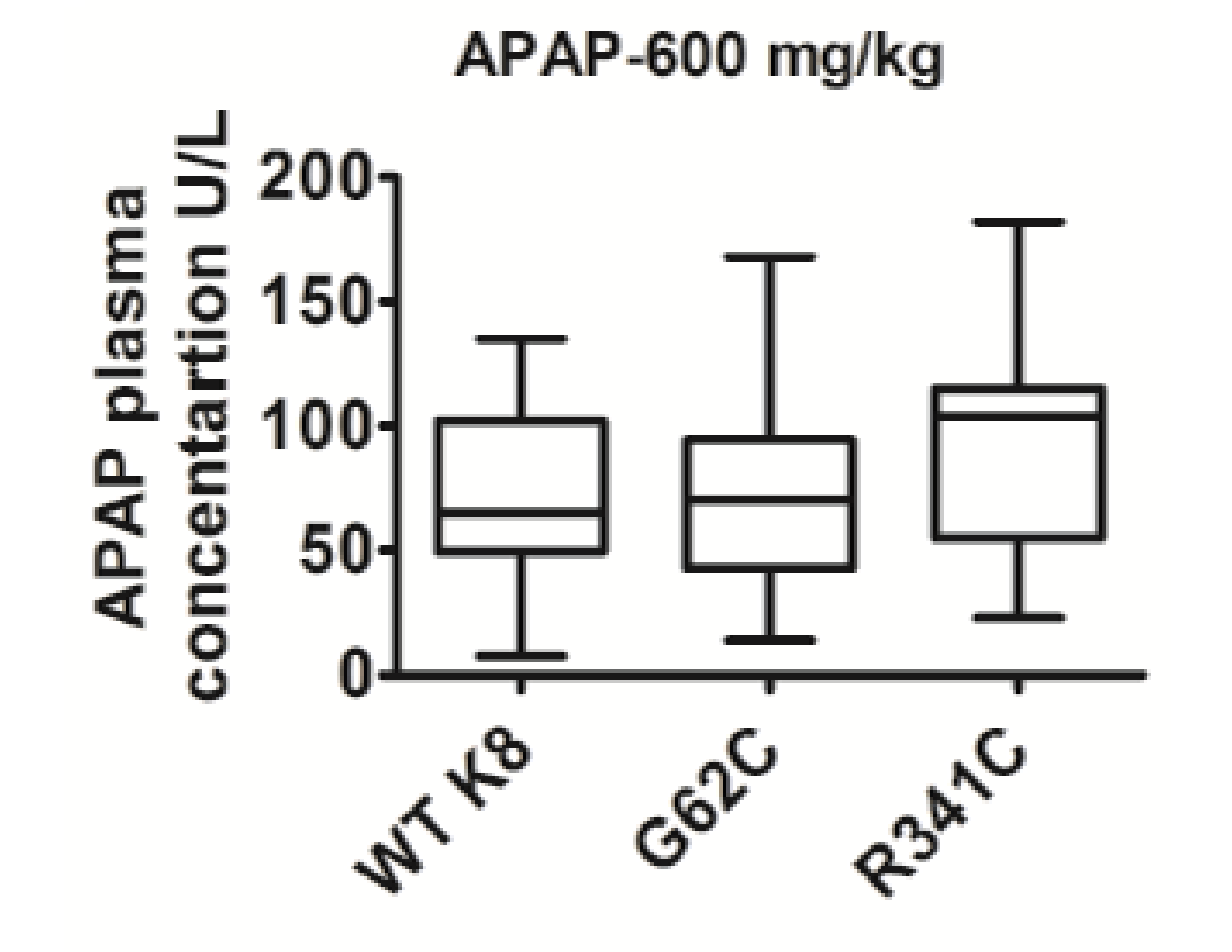
APAP-600 mg/kg
APAP plasma concentartion U/L
200
150
100
50
0
WT K8
G62C
R341C